Nuclear Instruments and Methods in Physics Research A 797 (2015) 37–43

Contents lists available at ScienceDirect

Nuclear Instruments and Methods in Physics Research A

journal homepage: www.elsevier.com/locate/nima

Thermal neutron flux monitors based on vibrating wire ☆

S.G. Arutunian [a], J. Bergoz [b], M. Chung [c], G.S. Harutyunyan [a], E.G. Lazareva [a]

[a] Yerevan Physics Institute, Alikhanian Br. St. 2, Yerevan 0036, Armenia
[b] Bergoz Instrumentation, 156 Rue du Mont Rond, 01630, France
[c] Ulsan National Institute of Science and Technology, Ulsan 689-798, Republic of Korea

ARTICLE INFO

Article history:
Received 25 March 2015
Received in revised form
2 June 2015
Accepted 5 June 2015
Available online 22 June 2015

Keywords:
Neutron
Detector
Vibrating wire
Gadolinium

ABSTRACT

Two types of neutron monitors with fine spatial resolutions are proposed based on vibrating wires. In the first type, neutrons interact with a vibrating wire, heat it, and lead to the change of its natural frequency, which can be precisely measured. To increase the heat deposition during the neutron scattering, the use of gadolinium layer that has the highest thermal neutron capture cross-section among all elements is proposed. The second type uses the vibrating wire as a "resonant target." Besides the measurement of beam profile according to the average signal, the differential signal synchronized with the wire oscillations defines the beam profile gradient. The monitor's spatial resolution is defined by the wire's diameter.

1. Introduction and overview

Many research centers in the world use neutrons as probes for investigating diverse properties of matter in different states (disordered, amorphous, glass, crystalline, non-equilibrium, and nanocomposite materials). Because neutrons are scattered by atomic nuclei, they provide information on the structure and dynamics of atoms and molecules over a wide range of length and time scales. Because neutrons possess magnetic moment, they can also be used for studying magnetic structures [1].

Neutrons have found interesting applications in medicine, both in the treatment of cancer and in the development of ultra-sensitive analytical techniques for studying the internal and external chemical environments of humans [2–6]. There are a few centers specializing in neutron therapy [7]. For these applications, controlling the spatial distribution and intensity of neutron beams is vital. In addition, devices capable of real-time acquisition/tracking of the neutron beam intensity are much needed.

Most of the existing neutron sources are based on nuclear reactors with strong time-averaged neutron flux and mature technologies (both source- and instrument-wise). Neutrons can also be generated at the so-called spallation facility, where neutrons are produced by bombarding a heavy nucleus target by a beam of energetic protons. Spallation sources can be either pulsed or continuous. Several new neutron sources are planned to become operational in the future.

Of great importance is forming the neutrons into a beam with strong flux, and obtaining well-identified and precisely controlled parameters of intensity, divergence, geometrical coordinates, and sizes. So far, neutron beams with fluxes of 10^{13}–10^{15} n/cm^2/s have been obtained. The new and important task is to achieve neutron beams with higher intensity.

Neutron beams require a variety of detectors and monitors for measuring and controlling. Today, all known detectors for slow neutrons are based on the conversion of neutrons into charged particles/photons (see e.g. [8]). After this conversion, the following technologies are normally used: gas proportional counters, ionization chambers, scintillation detectors, and semiconductor detectors. As conversion materials, He, Li, B, and Gd are often used owing to their high nuclear reaction cross-sections. In most cases, information on the spatial distribution of a neutron beam is also necessary.

For neutron beam measurements, we suggest a novel method based on the heat release by neutrons in a wire. The proposed novel detectors have fine spatial resolution defined by the wire diameter, ranging from 10 to 200 μm. We intend to combine two unique properties – the unprecedented sensitivity of the natural frequency of a clamped vibrating wire to the wire temperature, and remarkable neutron-capturing ability of several gadolinium isotopes. The dependence of frequency on the wire temperature was used as the operational principle of the vibrating wire monitors for beam diagnostics in accelerators [9–11]. The characteristic mode of natural oscillation in the wire is generated by the interaction of an AC drive current through the wire with a permanent magnetic field [12]. A special feedback scheme selects the resonant frequency at which AC current frequency is equal to the wire's natural frequency. A microcontroller measures the

☆The authors are grateful to Prof. T. Reetz for his friendly help.
E-mail addresses: femto@yerphi.am (S.G. Arutunian), mchung@unist.ac.kr (M. Chung).

http://dx.doi.org/10.1016/j.nima.2015.06.008
0168-9002/

frequency with 0.01 Hz resolution at 1 s sampling. A frequency shift arises when the beam particles penetrate the wire and change the wire temperature. For charged particles, ionization loss is the main contributor to the energy transfer.

The vibrating wire technology was first applied for measuring low-current electron beams in the injector of Yerevan synchrotron [9]. The principle of the operation was to measure the frequency shift of natural frequency of a stretched wire exposed to the beam. Even a small number of electrons penetrating the wire were sufficient for producing a detectable change of frequency. Since then, many other applications using vibrating wires have been proposed. For example, it was demonstrated that very high sensitivity (minimum detectable temperature change as low as mK) could be achieved in the measurement of temperature shift. This feature was used for beam halo measurements (see e.g. [10,11]).

We propose to measure temperature increase of the wire containing gadolinium isotopes, which occurs when neutrons penetrate the wire and deposit some energy into the wire. To ensure efficient neutron capture, we plan to use composite wires with few layers. At the same time, the wire should have proper mechanical properties for obtaining high quality factor that defines the frequency measurement's accuracy. We primarily intend to utilize tungsten wires covered by a layer of gadolinium with different thicknesses. The proposed vibrating wire neutron monitor (VWNM) with composite wires and wide dynamic range can be used for precise profiling of high flux neutron beams from specialized neutron sources (research reactors and spallation sources) on the ends of the tubes that transport neutron beams to the numerous instruments. Different from the existing neutron measurement principles, the proposed method has high spatial resolution, depending on the wire diameter.

In the second method, we propose to use a vibrating wire oscillating at its fundamental mode as a moving target, by measuring neutron scattering at the wire's maximal deviation positions. To detect the beam of neutrons we intend to use gadolinium-covered wires. After the neutron capturing reaction, the neutron's binding energy is released as a cascade of gamma radiation, during the time interval of approximately 10^{-16} s [13,14]. If the neutron beam's flux varies along the distance approximately equal to the oscillation amplitude, the difference between the measurements of prompt gamma rays at subsequent extreme positions during the wire's oscillation can provide the information on the neutron beam gradient. To measure prompt gamma rays we intend to use nonselective scintillator detectors. Measurements of the differences in the prompt gamma-ray signals, synchronously with measuring the wire's oscillation frequency, will allow us to extract only neutron capture events from any homogeneous background of gamma rays with wide spectrum of energies.

The proposed method is aimed at profiling centimeter scale neutron beams with vibrating wires of a few centimeters long. For such wire sizes, the response times of the wire heating are too long (several seconds). The main advantage of the proposed resonant target approach is to reduce the measurement time down to $\sim$1 ms or less, which corresponds to the oscillation period of a few centimeter long wires.

Transverse beam profile measurement by using this method was tested with lightening the oscillating wire by using a laser beam [15]. Monitors of this type will be called resonant target vibrating wire neutron monitors (RT-VWNMs).

The developed monitors can be widely used in all applications of neutron beams. For example, the VWNM can be used as a precise monitor with excellent spatial resolution for high flux neutron beams in the specialized neutron sources with multi-branch infrastructure of numerous instruments for materials research. The RT-VWNM can be used as a robust and reliable instrument with excellent spatial resolution for diagnostics of low flux neutron beams (e.g. at the neutron therapy centers). Specialized multi-wire VWNM capable of rotating along the beam axis can be used for the recovery of complicated 2D profiles of large cross-section neutron beams in neutron tomography, imaging, and radiography.

For example, the VWNMs can be used in the 18 MeV cyclotron (Cyclone-18) of Yerevan's oncological center for direct beam profile measurements in medical treatment. Another area of use can be neutron beam diagnostics that is being planned to be generated at Cyclone-18 for use in a broad class of studies and experiments (engineering of materials, investigations of biological, chemical, and physical systems, astrophysics, nuclear physics, and materials science). Preliminary experiments and tests are planned to be performed on the ^{252}Cf spontaneous fission neutron source accessible in Yerevan Physics Institute.

2. Neutron sources and detectors

Most of the existing neutron sources are based on nuclear reactors. Nuclear reactors use the fission process to produce neutrons. Most of the current reactor sources for scattering applications were primarily designed for materials testing for the nuclear industry [16].

Neutrons can also be generated at the so-called spallation facility, where neutrons are produced by bombarding a heavy nucleus target by a beam of energetic protons. Spallation sources can be either pulsed or continuous. Several new neutron sources are planned to become operational in the future [16].

To illustrate more clearly the complicated and manifold structure of the specialized neutron sources, we present detailed information on a reactor-based neutron source, hi-flux advanced neutron application reactor (HANARO) [17].

The main parameters of HANARO are as follows [18]:

Reactor power	30 MW
Max thermal flux	5×10^{14} n/cm^2/s
Typical flux at port nose	2×10^{14} n/cm^2/s
7 horizontal ports and 36 vertical holes	

The tubes and holes, as well as the positions of the instruments available at HANARO reactor, are shown in Fig. 1.

The design characteristics of the neutron fluxes at HANARO reactor are presented in Table 1 [19].

In Table 2, we list some other existing neutron sources in the world, with brief description of the source type and parameters, main characteristics of the generated neutron beam, and listing of some instruments with the values of fluxes [20–26].

Neutrons can also be produced by spontaneous fission [16]. Higher intensities can be achieved by using small accelerator-based neutron sources. Sealed tube sources with a typical length of 1 m and diameter of 10 cm, operating at a power of 0.5 kW, can produce up to 3×10^{10} n/s.

Because neutrons are neutral particles and do not ionize the matter directly, straightforward detection of these particles is impossible. Thus, most detection approaches rely on detecting various reaction products [27]. Any neutron–nucleus interaction leaves the nucleus in an excited state from which it decays by emitting gamma rays. Prompt gammas are emitted within 10^{-13} s and are always associated with the neutrons moving in the matter. The energy of prompt gamma rays depends on the neutrons energy. In gas detectors, a typical reaction involves a chamber filled with Helium 3. In the ionization mode of a gas detector, electrons drift to the anode, producing a charge pulse and the

corresponding signal. In the proportional mode, high voltage is applied so that electron–gas collisions ionize the gas atoms, yielding even more electrons. In scintillation detectors, converting medium is a scintillator that produces numerous photons as a result of neutron reaction. Photomultipliers are commonly used following the production of photons.

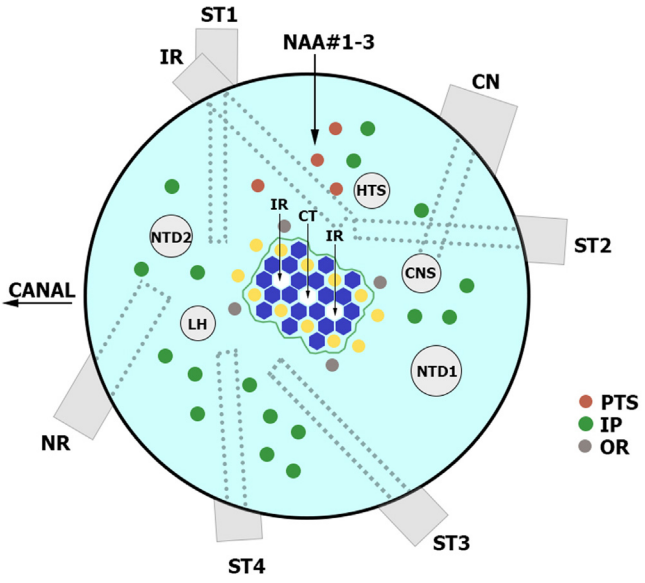

Fig. 1. Horizontal section of high-flux advanced neutron application reactor (HANARO) with description of the positions of instruments, tubes, and holes: PTS – pneumatic transfer system for neutron activation, IP – radioisotope production, OR – capsule irradiation and radioisotope production, IR – ex-core neutron irradiation facility for BNCT and dynamic neutron radiography, CT – capsule irradiation and radioisotope production, HTS – hydraulic transfer system for radioisotope production, NTD1 and NTD2 – neutron transmutation doping of silicon, LH – large hole, CNS – cold neutron source, NR – neutron radiography facility, ST1 – prompt gamma activation analysis, NAA#1–3 – neutron activation analysis, CN – cold neutron guide, ST2 – high-resolution power diffractometer, ST3 – bio diffractometer, high-intensity powder diffractometer, ST4 – triple axis spectrometer.

Table 1
Fluxes at the ends of beam tubes.

Beam tube	Thermal neutron flux, ($\times 10^{14}$ n/cm^2/s)	Total neutron flux, ($\times 10^{14}$ n/cm^2/s)
ST1	1.892	2.262
ST2	2.216	2.507
ST3	2.242	2.523
ST4	1.532	1.691
NR	0.432	0.440
IR	2.702	3.449
CN	0.968	1.004

3. Vibrating wire neutron monitor (VWNM) with composite wires – direct thermal measurements

Among all stable isotopes in the periodic table, the ^{157}Gd isotope has the highest cross-section for capturing thermal neutrons. The ^{155}Gd and ^{157}Gd isotopes absorb neutrons in a wide range of energies: ^{155}Gd has 104 resonant levels in the 0.0268–168 eV range, and ^{157}Gd has 60 resonant levels in the 0.0314–307 eV range [28]. Thus, the ^{157}Gd capture reaction initiates complex inner shell transitions that generate prompt γ emission, displacing an inner core electron. This electron in turn induces internal conversion (IC) electron emission and finally Auger–Coster–Kronig electron emission along with soft X-ray and photon emissions.

The complete information of neutron capture cross-sections for isotopes of different elements is presented in [29]. For comparison, we note that ^{10}B has 3840 b, ^{16}O has 0.00019 b, ^{12}C has 0.0035 b, ^{1}H has 0.333 b, and ^{14}N has 1.83 b for neutron capture cross-sections.

To use this unprecedentedly high neutron capture capacity of gadolinium we proposed to cover vibrating wires by gadolinium layers. Such wires can be fabricated by magnetron sputtering of gadolinium on tungsten (see e.g. [30]). An alternative possibility is electrodeposition of gadolinium on tungsten electrodes in equimolar NaCl–KCl melt at 973 K [31] or in the molten LiCl–KCl eutectics [32]. According to the recommendation in [33] we intend to use a solution of $GdCl_3$ in LiClb (molar 59.5%)-KCl eutectic at 359 °C.

3.1. Gd neutron capture reaction, energy deposition

The Gd isotopes possess very different cross-sections of neutron capture, σ. In Table 3, we list the cross-section values for 0.025 eV thermal neutrons [34].

The cross-section for ^{157}Gd is 65 times greater than the cross-section of ^{10}B for capturing thermal neutrons. The thermal neutron capture by ^{157}Gd yields a cascade of gamma rays (one or more) with overall energy of 7.937 MeV. Overall, 390 lines with energy in the 79.5–7857.670 keV range, up to 139 gamma photons on 100 captured neutrons are emitted. Following the absorption of a neutron by the ^{157}Gd nucleus, for example, several isomeric transitions occur, resulting in the release of 3.288 photons on average. These photons have a wide range of energies with the mean of 2.394 MeV. A large number of internal conversion (IC) electrons are emitted owing to the large change in the angular momentum of the low-lying excited states of ^{158}Gd*. The Gd atoms

Table 2
Neutron sources.

Source name	Source type and neutron beam parameters
Oak Ridge Neutron Facility, High Flux Isotope Reactor HFIR	Reactor/power 85 MW; thermal neutron flux 2.6×10^{15} n/cm^2/s; different fluxes at different instruments in range of 10^7 n/cm^2/s–3×10^7 n/cm^2/s
Oak Ridge Neutron Facility, Spallation Neutron Source SNS	Spallation/1 GeV proton accelerator (1.4 mA); different fluxes at different instruments in range of 10^7 n/cm^2/s–10^9 n/cm^2/s
Frank Laboratory of Neutron Physics, Dubna, Russia, Reactor IBR-2	Reactor/mean power 2 MW; peak flux about 10^{16} n/cm^2/s in 1 ms interval (at 1850 MW peak power) [23]
Institute Laue-Langevin, Grenoble, France, High-Flux Reactor	Reactor/thermal power 58.3 MW; continuous neutron flux in the moderator region: 1.5×10^{15} n/cm^2/s
Paul Scherrer Institut PSI, Switzerland, SINQ	Spallation/590 MeV proton accelerator (current up to 2.3 mA); continuous flux of about 10^{14} n/cm^2/s
Kyoto University Research Reactor Institute, Kyoto, Japan, Reactor KURRI	Reactor/thermal power 5 MW; neutron flux in range of 8.2×10^{13}–3×10^{12} n/cm²/s, ^{10}B-neutron capture therapy (BNCT) flux about 10^9 n/cm²/s [26]

Table 3
Capture cross-sections for Gd isotopes.

	% in natural Gd	Cross-section, (b)	Cross-section, (cm^2)
Natural Gd	100	48,890	4.889E−20
^{152}Gd	0.2	1100	1.1E−21
^{154}Gd	2.2	90	9E−23
^{155}Gd	14.7	61,000	6.1E−20
^{156}Gd	20.6	2	2E−24
^{157}Gd	15.68	255,000	2.55E−19
^{158}Gd	24.9	2.4	2.4E−24
^{160}Gd	21.9	0.8	8E−25

relax to their ground states by emitting Auger electrons and characteristic X-rays (see [35]).

The characteristic length L of neutrons in gadolinium is defined by the following formula:

$$n\sigma L = 1, \tag{1}$$

where n is the density of Gd atoms. Setting the Gd atoms density to $\rho = 7.9$ g/cm^3 and atomic mass to $A = 157.25$ g/mol, we find $n = \rho/A/N_A = 3.03 \times 10^{22}$ cm^{-3}.

As it follows from Table 3 for thermal neutrons (0.025 eV) one can estimate $L = 6.7$ μm for natural Gd, and $L = 1.3$ μm for pure ^{157}Gd.

We developed two types of monitors: small-scale VWNM with ~10-μm-diameter tungsten wire and ~2-μm-thick Gd layer, and middle-scale VWNM with ~100-μm-diameter tungsten wire and ~10-μm-thick Gd layer. For the first type, we offer to employ ^{157}Gd that allows capturing all thermal neutrons falling on the wire. For the second type, it is possible to use natural Gd.

After the thermal neutron capture by Gd, the excited Gd atom returns to the ground state by releasing the binding energy (~7937 keV for ^{157}Gd) in the forms of prompt gamma rays, internal conversion X-rays, internal conversion electrons, and Auger electrons. Although the energy of the gamma rays is quite high, they contribute only a small part of their energy to the heat deposition. On the other hand, practically all the energy of internal conversion X-rays, internal conversion electrons, and Auger electrons, which constitutes only ~1% of the reaction binding energy, is converted into heat [36,37] (see also [38]). Therefore, for electrons and X-ray contributions, we use the value of 70 keV as a first approximation, according to [38]. It is important to note that the release of heat in the material occurs at a distance of a few μm, making the heat deposition the same for both small- and middle-scale monitors.

For the estimation of 7.9 MeV gamma-ray contributions, we should take into account that the absorption coefficient μ for tungsten is 8.63×10^{-1} cm^{-1} ($\mu/\rho = 4.47 \times 10^{-2}$ cm^2/g [39]). For a 100-μm-thick wire, it corresponds to the heat deposition of ~70 keV, and for a 10-μm-thick wire it corresponds to the heat deposition of ~7 keV.

Both mechanisms of heat contribution from one neutron lead to $\varepsilon_n = 140$ keV for middle-scale VWNM, and to 77 keV for small-scale VWNM, respectively.

3.2. Composite wire Gd VWNM

As a first approximation for the description of the Gd VWNM, let us consider a simplest one-wire model of vibrating wire monitor with the following parameters: d_W – the base wire diameter, l_W – the wire length, h – the Gd layer's thickness, l_A – the monitor aperture available for the neutron flux (indeed some neutrons can penetrate into the wire through the magnet system parts, which are neglected here). We note that the overall diameter of the vibrating wire is $d = d_W + 2h$, the base wire cross-section is $S_W = \pi d_W^2/4$, the Gd layer's cross-section is $S_{\mathrm{Gd}} = \pi h(d_W + h)$, the base wire volume is $V_W = S_W l_W$, and the Gd volume is $V_{Gd} = S_{Gd} l_W$.

We also introduce ρ_W – the density of the base wire material, and ρ_{Gd} – the density of the Gd layer; thus, the mean density of the composite wire is:

$$\rho = \rho_W \frac{1 + \rho_{Gd} V_{Gd}/\rho_W V_W}{1 + V_{Gd}/V_W}. \tag{2}$$

The second harmonic frequency of the wire at temperature T_0 is found from the following formulae:

$$F_0 = \frac{1}{l_W}\sqrt{\sigma_0/\rho}, \tag{3}$$

$$\Delta T = T - T_0$$

is

$$\frac{\Delta F}{\Delta T} = -\frac{(\alpha_W E_W S_W + \alpha_{\mathrm{Gd}} E_{\mathrm{Gd}} S_{\mathrm{Gd}}) F_0}{2\sigma_0 (S_W + S_{\mathrm{Gd}})}, \tag{4}$$

where E_W and E_{Gd} are the elasticity moduli of the wire material and of Gd, α_W is the wire material's coefficient of thermal expansion, and α_{Gd} is the same for Gd layer (one can compare Eq. (4) with the uniform wire formula $(\Delta F/\Delta T) = (E\alpha F_0/2\sigma_0)$ that was presented in [40], where E is the modulus of elasticity and α is the coefficient of thermal expansion of the uniform wire).

The wire's balance temperature T is found by noting that the power Q deposited into the wire is equal to the sum of contributions from all thermal sinks:

$$W = W_\lambda + W_{RAD} + \eta W_{CONV}, \tag{5}$$

where W_λ is the thermal conduction sink, W_{RAD} is the thermal radiation sink, and W_{CONV} is the thermal convection sink ($\eta = 1$ for the monitor in air and $\eta = 0$ for the monitor in vacuum).

The relation between the frequency shift of the vibrating wire and the measured neutron flux I_n is:

$$\frac{\Delta F}{I_n} = -\frac{(\alpha_W E_W S_W + \alpha_{Gd} E_{Gd} S_{Gd}) F_0 \varepsilon_n l_A (d + 2h)}{2\sigma_0 (S_W + S_{Gd})[8(\lambda_W S_W + \lambda_{Gd} S_{Gd})/l_W + 4\varepsilon\sigma_{ST\_B} T_0^3 \pi d l_W + \eta\alpha_{CONV}\pi d l_W/2]} \tag{6}$$

where λ_W and λ_{Gd} are the thermal conductivity coefficients of the base wire and Gd, respectively, σ_{ST_B} is the Stefan–Boltzmann constant, ε is the wire thermal emissivity and α_{CONV} is the coefficient of convective loss (in the estimation described below we introduce the experimentally measured value of 380 W/m^2/K [41]).

Eq. (4) defines the monitor's dynamic range. In our previous vibrating wire resonators, the maximal deviation of frequency was limited by 1000 Hz and the corresponding accuracy was 0.01 Hz. For small-scale VWNM, the dynamic range according to Eq. (4) is $\sim 3 \times 10^8$–3×10^{13} n/cm^2/s for air, and $\sim 8 \times 10^7$–8×10^{12} n/cm^2/s for vacuum. For middle-scale VWNM, the dynamic range is $\sim 2 \times 10^{10}$–2×10^{15} n/cm^2/s for air, and $\sim 10^9$–10^{14} n/cm^2/s for vacuum.

The above-mentioned values for the wire diameter and length give only typical scales of the VWNM dynamic range. The choice of the wire length depends mainly on the transverse size of a neutron beam. When the VWNM aperture can accommodate the entire beam size, the monitor will not interfere with the measured beam. We have experience of manufacturing the vibrating wire monitors up to 120 mm in length with aperture sizes up to 60 mm. The disadvantage of long wires is their increased response time. The small-scale VWNMs, on the other hand, have smaller response times but the spatial resolutions are rather low. Therefore, they can be used for the fast monitoring of the total neutron flux at the monitor's local position.

The VWNM response time is defined as follows:

$$\tau = \frac{l_W(S_W \rho_W c_W + S_{Gd} \rho_{Gd} c_{Gd})}{8(\lambda_W S_W + \lambda_{Gd} S_{Gd})/l_W + 4\varepsilon\sigma_{ST\_B} T_0^3 \pi d l_W + \eta\alpha_{CONV}\pi d l_W/2} \tag{7}$$

For small-scale VWNM, the response time in air is ~15 ms while the response time in vacuum is ~70 ms. For middle-scale VWNM, the response times are ~0.3 s and ~3 s for air and vacuum, respectively.

Schematic presentations of the middle-scale and small-scale monitors are shown in Fig. 2. The important component of the vibrating wire monitors is their magnetic field system that produces mechanical forces exciting the wire vibration. In the middle-scale VWNMs, magnetic field is produced by samarium–cobalt permanent magnets placed at iron magnetic poles. In this case, the monitor aperture is defined by the opening between these poles. In the small-scale VWNMs, the wire is placed right on the surface of only one permanent magnet without covering it by the poles. Thus, the entire length of the wire becomes open for the measured beam.

The problem of radiation damage thresholds for permanent magnets was investigated, for example, in [42]. Different types of commercially important magnet materials were irradiated to integrated neutron flux level up to 4×10^{20} n/cm^2. In spite of this relatively high dose all type of magnets showed negligible change in properties. It means that the lifetime of the magnet system should be longer 230 days at the intensity level 1000-fold of the minimal detectable flux for middle-scale VWNM, and even much longer for small-scale VWNM owing to the lower flux.

As a positioning mechanism we intend to use high-precision one-dimensional feeding system for middle-scale monitors, and 2D positioning system for small-scale VWNM.

As one can see from Eqs. (6) and (7), the resolution and response time of the VWNM depend essentially on the wire length and diameter. By reducing these parameters, the resolution and the response time can also be reduced. For a ~10-μm-diameter tungsten wire and a ~2-μm-thick natural Gd layer, a ~5-mm-long wire can be placed in the magnetic field of the permanent magnet below the wire. So the aperture of the monitor can also be defined as ~5 mm.

Each neutron capture process by gadolinium isotopes with large cross-sections (^{155}Gd and ^{157}Gd) converts gadolinium to the practically "dead" ones (^{156}Gd and ^{158}Gd correspondingly). The number of all Gd atoms in the wire aperture volume is 2×10^{18} for a typical middle-scale VWNM. Thus, the lifetime at the intensity level 1000-fold of the minimal detectable flux is about 60 days. For small-scale VWNM, the estimated lifetime of the monitor is more than one year owing to the lower flux.

The small-scale VWNM may be used in the field of nuclear safety as a portable, high-speed environmental monitor.

The middle-scale VWNM can have sufficiently large aperture for neutron beam profiling with precise spatial resolution.

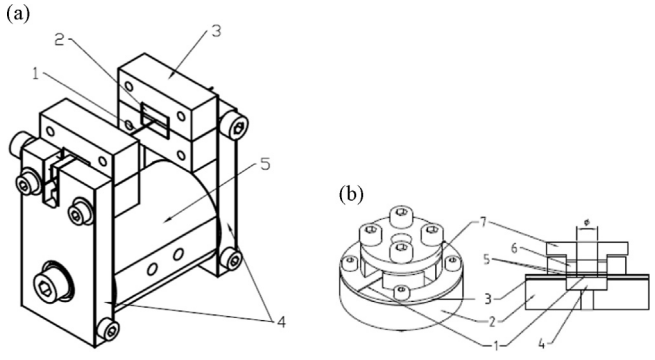

Fig. 2. Schematic sketches of (a) middle-scale VWNM: 1 – vibrating wire, 2 – magnets, 3 – magnet poles, 4 – clips, 5 – base, and (b) small-scale VWNM: 1 – vibrating wire, 2 – support base, 3 – wire contacting washer, 4 – magnet, 5 – two thin washers from ceramics, washer with or without hole, 6 – elastic washer, 7 – clamping washer from magnetic material.

4. Resonant target vibrating wire neutron monitor (RT-VWNM)

In this section, we suggest a new method for measuring flux gradients of neutron beams. The core of the method consists in using the vibrating wire as a moving target at different positions during the oscillation process. Normally the oscillation's amplitude is on order of the wire diameter. During the neutrons scattering, the amount of secondary particles and radiation is proportional to the number of neutrons captured by the wire. If the flux gradient of the neutron beam is observable along the distance on the order of the oscillation amplitude, the difference between the measured levels of the particles/radiation can provide a signal proportional to the gradient of the neutron beam distribution. To be able to perform this measurement, the measurement needs to be in resonance with the vibrating wire frequency. Eventually, we should measure the scattered particles/radiation during a short time (much shorter than the wire's oscillation period), synchronously with the extreme positions of the wire during the mechanical oscillation process. For increasing the area swept by the wire, it is preferable to use the oscillation's first harmonic.

The method was tested by using a laser beam and fast photodiodes measuring the scattered photons from the opposite positions of the wire's maximal deviation relative to the straight line [15]. A 100-μm-diameter and 80-mm-long stainless steel wire was used, and it oscillated with the stable amplitude of ~200 μm (peak to peak). Results of this experiment are presented in Fig. 3. In Fig. 3, we observe three different approaches to the beam profiling. Dark blue and light blue lines indicate that the measurements of the vibrating wire frequency depend on the deposition of heat from the measured beam, and environmental conditions lead to signal drifts. The absolute photodiode signal (red and magenta lines) does not require the oscillation process and can be obtained even without the wire vibration. However, the signal of the measured beam contains some additional background. In our case the background is ~500 mV and the excess of useful signal is quite high, i.e., ~2000 mV, but in other cases the background can be significantly larger. In the resonant target method, the background is completely removed by subtracting it, and the signal outside the beam becomes zero (green and brown lines).

For this experiment, we manufactured home-made electronics with measurement gates and delays, which were correlated with the wire oscillation frequency. This precise measurement technique allowed obtaining the measurements accuracy in the mHz range, within 1-s-long sampling interval. Another possibility is applying special electronic devices for signal extraction in a narrow gap around the oscillation frequency – the so-called lock-in amplifier with unprecedented small filtering gap.

Lock-in amplifiers are used for detecting and measuring very small AC signals. In our case, the reference frequency should be the vibrating wire's frequency. It is important to notice that the short-term frequency stability of the vibrating wire monitors is less than 0.01 Hz, allowing to apply a filter with passband of the same order.

For neutron beam measurements, we propose to use popular NaI(Tl) scintillator-based detectors with photomultiplier tubes. In principle, such detectors can detect even a single photon owing to their very high multiplication factors (up to 10^6). Because of the differential principle of the measurements, we can use the total integral response of the detector during data acquisition without temporally separating the individual pulses. The signal should be sufficiently strong for picking out the difference between the photons emitted during the opposite phases of the wire oscillation. The measurement system is sufficiently fast: the decay constant of NaI is 0.23 μs and the overall time constant of the system does not exceed a few μs, including the response time of a preamplifier of the photomultiplier tube.

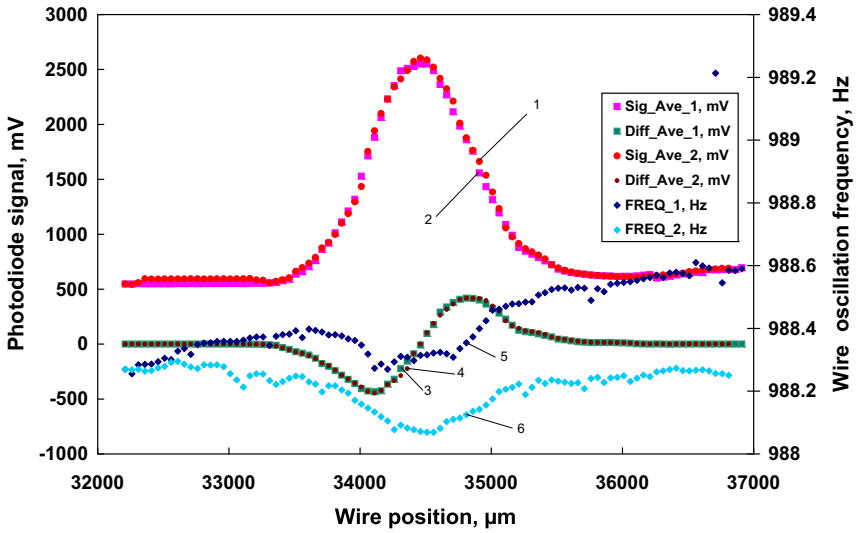

Fig. 3. Measurement results obtained by using a laser beam, as functions of the wire's scanning position. Red (1, squares) and magenta (2, circles) lines – the averaged absolute signal from the photodiode (forward and backward scans), green (3, squares) and brown (4, circles) lines – the differential signal from the photodiode (forward and backward scans), dark blue (5, diamonds) and light blue (6, diamonds) lines – the frequency signal (forward and backward scans). (For interpretation of the references to color in this figure legend, the reader is referred to the web version of this article.)

The advantage of the proposed resonant target vibrating wire neutron monitor (RT-VWNM) is that the speed of operation is faster than that of the VWNM. For RT-VWNM, the speed of operation is defined by the wire oscillation period, which is below 1 ms. In particular, the proposed method can be useful in the presence of a strong background. In addition, the measurements can be complemented by acquiring the absolute signals coming from the scattering, and by sampling the wire oscillation frequency that represents the wire temperature change.

The presented results of the gradient measurements were obtained by using the laser beam with transverse size on the millimeter scale. In the case of neutron beams with transverse sizes of a few centimeters or larger, it is preferable to use longer wires with oscillation amplitudes about three or more times of the wire diameter.

The complete design depends on the specific parameters of neutron beam and VWNM. Here, as an example, we present an estimation using typical numbers. Suppose we intend to measure a neutron beam with 10^7 n/cm^2/s flux by using RT-VWNM with 200-μm-diameter and 100-mm-long wire. Then, a resonator with natural oscillation frequency of ~800 Hz and oscillation amplitude on the order of 0.6 mm can be prepared. During the half period of the oscillation ~3130 neutrons are scattered. This scattering leads to ~4340 photons. We can consider two measurement possibilities. For the measurements outside of vacuum chamber, a NaI detector with aperture of 5 cm × 5 cm can be placed at a distance of 2.5 cm from the wire. In this case, the detector is expected to accept about 1380 photons during the measurement time. As a first approximation, we assumed that the difference between subsequent measurements is about $\sqrt{1380} = 37$ resolved photons. This difference corresponds to the gradient resolution of ~37/1380/0.6 mm = 0.22 cm^{-1}. This implies that by using the proposed method we can measure the gradient of a ~4.5-cm-wide neutron beam. For the measurements inside the vacuum chamber, the distance of the NaI detector from the wire would be of order of the vacuum chamber sizes, e.g. 5–10 cm. In this case the RT-VWNM gradient resolution should be about 0.44–0.9 cm^{-1} (this corresponds to the measurements of 1–2.5 cm-wide neutron beams).

5. Conclusion

The main advantage of the proposed instruments, VWNM and RT-VWNM, is that they allow measuring profiles of thermal neutron fluxes with excellent spatial resolutions. At the same time, they are simple, robust, and radiation-resistant devices that can operate in difficult conditions. It is important to note that properly constructed vibrating wire monitors have inherent long term stability, negligible zero drift, high precision and resolution, good reproducibility, and small hysteresis. Vibrating wire monitors produce frequency signals that are interference-protective and can be transmitted over long cables without loss or degradation. Taking into account that VWNM and RT-VWNM can cover a wide range of neutron beam flux intensities, we can confidently state that the proposed vibrating-wire based neutron monitors can be widely used in all applications of neutron beams. Further, small-scale VWNM may be used in the field of nuclear safety as a portable, high-speed environmental monitor.

A specialized multi-wire VWNM with the capability of rotating along the beam axis could be used for the recovery of complicated 2D profiles of large cross-section neutron beams in neutron tomography, imaging, and radiography.

The VWNMs can be used in the 18 MeV cyclotron (Cyclone-18) of Yerevan's oncological center for direct beam profile measurements in medical treatment. Another area of use can be diagnostics of neutron beam planned to be generated at Cyclone-18. Preliminary experiments and tests are planned by using spontaneous fission neutron sources available in Yerevan Physics Institute.

Besides the concept of the VWNM, a general overview of the neutron sources and associated instruments can be found in [43].

References

[1] ESS Technical Design Report, Ess-doc-274, 23 April 2013.
[2] R.C. Lawson, J.M.A. Lenihan, Physics in Technology 13 (1982) 233.
[3] W.A.G. Sauerwein, A. Wittig, R. Moss, Y. Nakagawa, Neutron Capture Therapy: Principles and Applications, Springer-Verlag, Berlin, Heidelberg (2012) 554.
[4] Y. Mishima (Ed.), Cancer Neutron Capture Therapy, Plenum Press, New York, 1996, p. 920.
[5] R.F. Barth, D.E. Carpenter, A.H. Soloway, Advances in Neutron Capture Therapy, Springer (2013) 830.
[6] N.S. Hosmane, J.A. Maguire, Y. Zhu, M. Takagaki, Boron and Gadolinium Neutron Capture Therapy for Cancer Treatment, World Scientific (2012) 272.
[7] A.N. Dovbnya, E.L. Kuplennikov, S.S. Kandybey, V.V. Krasiljnikov, Physics of Elementary Particles and Atomic Nuclei 45 (5–6) (2014) 1749 (in rus.).
[8] L.V. Tarasov, Low-Energy Neutron Physics, North-Holland Pub. Co. (1968) 608.
[9] S.G. Arutunian, N.M. Dobrovolski, M.R. Mailian, I.G. Sinenko, I.E. Vasiniuk, Physical Review Special Topics, Accelerators and Beams 2 (1999) 122801.

[10] S.G. Arutunian, A.E. Avetisyan, N.M. Dobrovolski, M.R. Mailian, I.E. Vasiniuk, K. Wittenburg, R. Reetz, Problems of Installation of Vibrating Wire Scanners into Accelerator Vacuum Chamber, in: Proceedings of the 8-th European Particle Accelerator Conference, Paris, France, 2002, pp. 1837–1839.
[11] S.G. Arutunian, M. Werner, K. Wittenburg, Beam tail measurements by wire scanners at DESY, in: Proceedings of ICFA Advanced Beam Dynamic Workshop: Beam HALO Dynamics, Diagnostics, and Collimation, HALO'03 (in conjunction with 3rd workshop on Beam–beam Interaction), Gurney's Inn, Montauk, NY USA, May 19–23, 2003, AIP Conf. Proceedings, (2003) 129–132.
[12] S.G. Arutunian, A.E. Avetisyan, M.M. Davtyan, G.S. Harutyunyan, I.E. Vasiniuk, M. Chung, V. Scarpine, Physical Review Special Topics, Accelerators and Beams 17 (2014) 032802.
[13] Z. Révay, T. Belgya, in: G.L. Molnar (Ed.), Handbook of Prompt Gamma Activation Analysis with Neutron Beams, Kluwer Academic, Publishers, Dordrecht, 2004, pp. 71–111.
[14] S. Söllradl, Developments in prompt gamma-ray neutron activation analysis and cold neutron tomography and their application in non-destructive testing, Inauguraldissertation der Philosophisch-naturwissenschaftlichen Fakultät der Universität Bern, 2014. ⟨http://www.psi.ch/lch/AlumniEN/Sollradl_Thesis_PSIuUniBern_2014.pdf⟩.
[15] S.G. Arutunian, A.V. Margaryan, Oscillating wire as a "Resonant Target" for beam transversal gradient investigation, in: Proceedings of International Particle Accelerator Conference, IPAC2014, Dresden, Germany, 2014, pp. 3412–3414.
[16] M. Arai, K. Crawford, Neutron sources and facilities, in: I.A. Anderson, R. L. McGreevy, H.Z. Bilheux (Eds.), Neutron Imaging and Applications: A reference for the Imaging Community, Springer Science+Business media, New York, 2009, pp. 13–30.
[17] K.H. Lee, J.M.S. Park, H.-R. Kim, B.J. Jun, Y.-J. KIM, J.-J. Ha, Nuclear Engineering and Technology 41 (4) (2009) 521.
[18] Cho Man Soon, HANARO projects, VIC F0185, IAEA, Vienna, 10–12 June, 2013.
[19] H. Kim, H.R. Kim, K.H. Lee, J.B. Lee, Journal of Nuclear Science and Technology 33 (7) (1996) 527.
[20] ⟨http://neutrons.ornl.gov/instruments/HFIR/⟩.
[21] T.E. Mason, D. Abernathy, I. Anderson, J. Ankner, T. Egami, G. Ehlers, A. Ekkebus, G. Granroth, M. Hagen, K. Herwig, J. Hodges, C. Hoffmann, C. Horak, L. Horton, F. Klose, J. Larese, A. Mesecar, D. Myles, J. Neuefeind, M. Ohl, C. Tulk, X.L. Wang, J. Zhao, Physica B: Condensed Matter 385–386 (2006) 955.
[22] ⟨http://lansce.lanl.gov/lujan/index.shtml⟩.
[23] M Frontasyeva, Neutron News 16 (3) (2005) 24.
[24] ⟨http://www.ill.eu/reactor-environment-safety/high-flux-reactor/technical-characteristics/⟩.
[25] ⟨http://www.psi.ch/sinq/instrumentation⟩.
[26] Y. Sakurai, T. Fujii, R. Uchida H. Tanaka, Establishment of QA/QC for BNCT Neutron Irradiation Field, in: KURRI Progress Report 2012.
[27] T.E. Mason, Neutron Detectors for Materials Research, ⟨http://fire.pppl.gov/neutron_detectors_aug_00.ppt⟩.
[28] A.A. Poljakov, Ju.V. Stogov, L.N. Jurova, Computational experimental studies of resonant absorption of neutrons in the fuel element of the water-moderated water-cooled power reactors containing oxide uranium–gadolinium fuel, ⟨http://www.library.mephi.ru/data/scientific-sessions/1999/5/219.html⟩ (in rus).
[29] S.F. Mughabghab, Atlas of Neutron Resonances, Academic Press (2006) 1005.
[30] A. Heysa, P.E. Donovan, A.K. Petford-Long, R. Cywinski, Journal of Magnetism and Magnetic Materials 131 (1–2) (1994) 265.
[31] H.B. Kushkhov, A.S. Uzdenova, M.M.A. Saleh, A.M.F. Qahtan, L.A. Uzdenova, American Journal of Analytical Chemistry 4 (2013) 39.
[32] C. Caravaca, G. de Cyrdoba, M.J. Tombs, M. Rosado, Journal of Nuclear Materials 360 (1) (2007) 25.
[33] Teja Reetz, Private communication.
[34] ⟨http://arxiv.org/ftp/physics/papers/0611/0611225.pdf⟩.
[35] D. Bufalino, N. Cerullo, V. Colli, G. Gambarini, G. Rosi, Journal of Physics: Conference Series 41 (2006) 195.
[36] P. Kandlakunta, L.R Cao, P Mulligan, Nuclear Instruments and Methods in Physics Research A 705 (2013) 36.
[37] P. Kandlakunta, A Proof-of-Principle Investigation for a Neutron-Gamma Discrimination Technique in a Semiconductor Neutron Detector (M. Sc thesis), Graduate School of The Ohio State University, 2012.
[38] S.A. Klykov, The reaction of Gd (n, γ) as a source of ionizing radiation for neutron capture therapy, Scientific Library of dissertations and author's abstract, ⟨http://www.dissercat.com/content/reaktsiya-gdng-kak-istochnik-ioniziruyushchego-izlucheniya-dlya-neitron-zakhvatnoi-terapii#ixzz3UMKn433o⟩ (in rus.).
[39] ⟨http://physics.nist.gov/PhysRefData/XrayMassCoef/ElemTab/z74.html⟩.
[40] S.G. Arutunian, N.M. Dobrovolski, M.R. Mailian, I.E. Vasiniuk, Physical Review Special Topics, Accelerators and Beams 6 (2003) 042801.
[41] S.G. Arutunian, G. Decker, M.R. Mailian, G. Rosenbaum, Transition thermal processes in vibrating wire monitor, in: Proceedings of the 8th European Workshop on Beam Diagnostics and Instrumentation for Particle Accelerators, DIPAC 2007, Venice, Italy, 2007, pp. 292–94.
[42] R.S. Sery, R.H. Lundsten, D.I. Gordon, Radiation damage thresholds for permanent magnets, NOLTR 61-45, United States Naval Ordnance Laboratory, White Oak, Maryland, 18 May 1961. ⟨http://www.researchgate.net/publication/235054786_RADIATION_DAMAGE_THRESHOLDS_FOR_PERMANENT_MAGNETS⟩.
[43] S.G. Arutunian, J. Bergoz, M. Chung, G.S. Harutyunyan, E.G. Lazareva, Proposal of thermal neutron flux monitors based on vibrating wire, arXiv:1502.04050.